AD-A212 850

REPORT DOCUMENTATION PAGE

Form Approved
OMB No. 0704-0188

1a. REPORT SECURITY CLASSIFICATION	1b. RESTRICTIVE MARKINGS
Unclassified	

2a. SECURITY CLASSIFICATION AUTHORITY	3. DISTRIBUTION/AVAILABILITY OF REPORT
2b. DECLASSIFICATION/DOWNGRADING SCHEDULE	Approved for public release; distribution unlimited.

4. PERFORMING ORGANIZATION REPORT NUMBER(S)	5. MONITORING ORGANIZATION REPORT NUMBER(S)
HDL-TR-2162	

6a. NAME OF PERFORMING ORGANIZATION	6b. OFFICE SYMBOL (If applicable)	7a. NAME OF MONITORING ORGANIZATION
Harry Diamond Laboratories	SLCHD-ST-AP	

6c. ADDRESS (City, State, and ZIP Code)	7b. ADDRESS (City, State, and ZIP Code)
2800 Powder Mill Road Adelphi, MD 20783-1197	

8a. NAME OF FUNDING/SPONSORING ORGANIZATION	7b. OFFICE SYMBOL (If applicable)	9. PROCUREMENT INSTRUMENT IDENTIFICATION NUMBER
U.S. Army Laboratory Command	AMSLC	

8c. ADDRESS (City, State, and ZIP Code)	10. SOURCE OF FUNDING NUMBERS			
	PROGRAM ELEMENT NO.	PROJECT NO.	TASK NO.	WORK UNIT ACCESSION NO.
2800 Powder Mill Road Adelphi, MD 20783-1145	611102.H4400	AH44		

11. TITLE (Include Security Classification)

Elastic Impurity Scattering in Double-Barrier Resonant Tunneling Structures

12. PERSONAL AUTHOR(S)
Thomas B. Bahder and John D. Bruno

13a. TYPE OF REPORT	13b. TIME COVERED	14. DATE OF REPORT (Year, Month, Day)	15. PAGE COUNT
Final	FROM July 88 TO Jan 89	September 1989	28

16. SUPPLEMENTARY NOTATION
AMS code: 611102.H440011; HDL Project No. AE1951

17. COSATI CODES			18. SUBJECT TERMS (Continue on reverse if necessary and identify by block number)
FIELD	GROUP	SUB-GROUP	Impurities, electron scattering, double-barrier structures, electron tunneling,
20	10		random impurities, quantum well, resonant tunneling, effective mass theory
20	12		

19. ABSTRACT (Continue on reverse if necessary and identify by block number)

Fermi's golden rule is used to calculate the electron elastic scattering rate due to a single charged impurity in the quantum well region of a double-barrier resonant tunneling structure at zero applied electric field. The impurity is modelled by a screened Coulomb potential, and the scattering rate out of a conduction band eigenstate is calculated as a function of the initial-state electron wave vector and the impurity position. In a finite crystal with a random distribution of impurities, the scattering of resonant electrons can be dominated by impurities in the quantum well region. For a double-barrier structure embedded in an infinite crystal, impurity scattering of resonant electrons is always dominated by impurities outside the quantum well region.

20. DISTRIBUTION/AVAILABILITY OF ABSTRACT	21. ABSTRACT SECURITY CLASSIFICATION
☒ UNCLASSIFIED/UNLIMITED ☐ SAME AS RPT. ☐ DTIC USERS	Unclassified

22a. NAME OF RESPONSIBLE INDIVIDUAL	22b. TELEPHONE (Include Area Code)	22c. OFFICE SYMBOL
Thomas B. Bahder	(202) 394-2042	SLCHD-ST-AP

DD Form 1473, JUN 86   Previous editions are obsolete.

Contents

Figures

1. Introduction

Advances in molecular beam epitaxy and other crystal growth techniques have allowed detailed studies of semiconductor heterostructures [1].* In the last few years, the double-barrier resonant tunneling structure has been studied by a number of groups. This structure consists of a thin layer of GaAs (about 50 Å) surrounded on both sides by a layer of AlGaAs (of similar thickness), all embedded in a GaAs crystal. When electrically contacted and biased, this structure displays peaks in its current-voltage characteristic [2-13]. From the scattering point of view, these peaks are attributed to peaks in the transmission coefficient [14]. In terms of the electronic structure, the double-barrier potential confines electronic states of certain energies, creating resonances that manifest themselves as peaks in the one-dimensional local density of states between the barriers [15-18]. For a symmetric structure in zero applied electric field, the states can be labelled by even or odd parity, $\alpha = e$ or o, a wave vector transverse to the growth direction, $\mathbf{k}$, and a wave vector along the growth direction, q, associated with the solution of a one-dimensional effective mass Schrödinger equation. The doubly degenerate electron energy eigenvalues are given by

$$E = \hbar^2(\mathbf{k}^2 + q^2)/2m_1, \tag{1}$$

where m_1 is the conduction band effective mass at the Γ-point (for GaAs). For a given value of $\mathbf{k}$, there are resonant values of q at which the amplitude of the wave function inside the quantum well region is large compared with the wave function amplitude outside this region. For wave vector values q that are not close to the resonant values, the amplitude of the wave function inside the quantum well region is suppressed relative to its outside value. Outside the quantum well region, the wave function amplitude is roughly the same for energies on- and off-resonance.

The above description of electronic states neglects certain aspects of the problem, such as external electric fields, scattering due to phonons [19], impurities, and electron/electron interactions. The effects of electron/electron interactions (space-charge buildup) on current-voltage characteristics have been discussed [20] and treated in detail within a self-consistent scheme [21]. Inelastic scattering, and its consequences for resonant tunneling, has also been discussed by several authors [18,22]. However, elastic scattering due to impurities has not been treated theoretically, despite the fact that at liquid nitrogen temperatures, where measurements on double-barrier structures are frequently made, elastic

*References are listed at the end of the main body of text.

scattering caused by charged impurities is the predominant scattering mechanism [23]. While it is true that elastic scattering events are not expected to have an effect on resonances that is comparable to inelastic events, recent experiments [13] on intentionally doped double-barrier structures show that their effect is nontrivial and needs to be better understood. In this paper we examine, in a qualitative way, the manner in which scattering rates from a single charged impurity depend upon the electron's initial state and the impurity's position. Next, assuming there is a distribution of randomly positioned impurities, we add the probability for scattering due to each impurity, resulting in a total elastic scattering rate. We find that for a finite system size and certain values of the parameters, such as impurity potential range, the scattering of resonant electrons (in the limit of low electric fields) can be dominated by impurities in the quantum well region. This is surprising because in circumstances where sharp resonances are absent, contributions from the quantum well region are the same order of magnitude as surface effects, which can be ignored.

In section 2 we establish our notation and briefly summarize the form of the electron eigenstates for a double-barrier potential. In section 3 we use these states to compute the scattering rate due to one impurity, and in section 4 we consider the effects of a random distribution of impurities.

2. Eigenstates

Within a one-band effective mass theory, an electron state is represented by a product wave function [24]

$$\Psi_{\alpha,\mathbf{k},q}(\mathbf{r}) = \psi_{\alpha,\mathbf{k},q}(\mathbf{r})u_c(\mathbf{r}) \equiv \langle \mathbf{r}|\alpha,\mathbf{k},q\rangle, \qquad (2)$$

where $u_c(\mathbf{r})$ is the conduction band Bloch function at the Γ-point (and is taken to be the same function for GaAs and AlGaAs), and $\psi_{\alpha,\mathbf{k},q}(\mathbf{r})$ are the envelope functions. For a double-barrier potential

$$V(z) = \begin{cases} V_o, & \text{if} \quad a < |z| < a(1+\delta); \\ 0 & \text{otherwise,} \end{cases} \qquad (3)$$

6

the envelope functions, normalized[*] to unity over a volume L^3, were previously calculated [17] and can be written

$$\psi_{\alpha,\mathbf{k},q}(\mathbf{r}) = \frac{1}{L}\exp(i\mathbf{k}\cdot\mathbf{r})\Phi_{\alpha,\mathbf{k},q}(z),\qquad(4)$$

where $\mathbf{k} = (k_x, k_y, 0)$, and α labels the parity of the state, $\alpha = e(o)$ for even (odd) parity. The z-dependent functions are given by

$$\Phi_{\alpha,\mathbf{k},q}(z) = \frac{F^{1/2}_{\alpha,\mathbf{k}}(qa)}{\sqrt{L/2}}\begin{cases}\cos(qz)\delta_{\alpha,e} + \sin(qz)\delta_{\alpha,o} & |z| \le a\\ d_\alpha(qa)\exp(w(qa)z/a) + e_\alpha(qa)\exp(-w(qa)z/a) & a \le z \le (1+\delta)a\\ f_\alpha(qa)\exp(iqz) + g_\alpha(qa)\exp(-iqz) & (1+\delta)a \le z \le L/2\end{cases}\qquad(5)$$

where $\delta_{\alpha,e}$ and $\delta_{\alpha,o}$ are Krönecker delta functions, and the auxiliary functions $d_\alpha(u)$, $e_\alpha(u)$, $f_\alpha(u)$, $g_\alpha(u)$, and $F_{\alpha,\mathbf{k}}(u)$ are defined in appendix A. The function $w(u)$ is given by

$$w(u) \equiv \sqrt{\frac{\tilde{\gamma} - u^2}{\beta}}\qquad(6)$$

and carries a dependence on transverse wave vector $\mathbf{k}$ through

$$\tilde{\gamma} \equiv \gamma - (1 - \beta)|\mathbf{k}|^2 a^2.\qquad(7)$$

Here, γ is the dimensionless barrier height given by $\gamma \equiv 2m_1 V_o a^2/\hbar^2$, and β is the ratio of the effective masses, $\beta \equiv m_1/m_2$, where m_1 is the mass in the quantum well region and outside the barriers, and m_2 is the mass in the barrier region. Because the effective mass in the quantum well region is different from that in the barrier regions, the effective barrier height, $\tilde{\gamma}$, is different for each $\mathbf{k}$.

The functions $\Phi_{\alpha,\mathbf{k},q}(z)$ and $(1/m)d\Phi_{\alpha,\mathbf{k},q}(z)/dz$ are continuous at the interfaces $z = \pm a$ and $z = \pm(1+\delta)a$. Periodic boundary conditions in a box of area $L \times L$ have been used in the x and y directions, so the allowed values of $\mathbf{k} = 2\pi(n_x, n_y, 0)/L$, where n_x and n_y can take any integer values. It is interesting to note that at sufficiently large $|\mathbf{k}|$, the effective barrier height may actually be negative. The allowed values of the z-component wave vector, q, are given by the roots of a transcendental equation whose precise form depends on the

---

[*]In normalizing the wave function, we have dropped terms of $O(a/L)$ and $O(a\delta/L)$. In the quantum well limit, $\gamma \to \infty$ or $\delta \to \infty$, the function $f_\alpha(qa)$ has zeros at resonant values of q, and the terms $O(a/L)$ and $O(a\delta/L)$ cannot be dropped. However, for any finite value of γ, there is always a large enough L so that dropping these terms is justified. Physically, this means we are neglecting surface effects, which can be important when the thickness of the crystal becomes sufficiently small, or when we approach the $\gamma \to \infty$ or $\delta \to \infty$ limit, with L fixed.

boundary conditions at $z = \pm L/2$. However, in the limit $a/L \to 0$, the density of roots approaches $L/2\pi$, and the solution of this equation is not necessary. The energy eigenvalues associated with the state given by equation (2), measured from the bottom of the conduction band, are given by equation (1).

The envelope functions given in equation (4) contain the resonance effects due to the presence of the double-barrier potential through the functions $F_{e,\mathbf{k}}(u)$ and $F_{o,\mathbf{k}}(u)$. For a given $\mathbf{k}$, these functions have peaks at $u = qa$, for wave vector values $q = q_{e,1}$, $q_{e,2}$, $q_{e,3}$, ..., and $q_{o,1}$, $q_{o,2}$, $q_{o,3}$, ..., respectively. The peaks in these functions correspond to an even and an odd series of resonances. These functions are intimately related to the local density of states, and have been discussed in detail elsewhere [17]. An electron with a given transverse wave vector, $\mathbf{k}$, and q close to a resonant value has a wave function with a large amplitude in the quantum well region and, correspondingly, a decreased amplitude outside the barriers, so that normalization over the interval $(-L/2, +L/2)$ is maintained.[†] An electron whose wave vector is not near resonance has a small wave function amplitude in the quantum well and barrier regions and, correspondingly, a larger amplitude outside these regions. Figure 1 shows a plot of the square of the even envelope function, $|\psi_{e,\mathbf{k},q}(\mathbf{r})|^2$, versus z/a, for on-resonance and off-resonance electron states. The state that has a wave vector in the resonance region, $qa = 0.80$, has a large wave function amplitude in the well, compared to a state whose wave vector lies outside the resonance range, $qa = 1.5$.

When the resonances are quite sharp it is appropriate to speak about resonant subbands, analogous to the two-dimensional subbands in a quantum well structure. A resonant subband is defined by a resonant value of q (equal to one of the $q_{e,1}$, $q_{e,2}$, $q_{e,3}$, ..., or $q_{o,1}$, $q_{o,2}$, $q_{o,3}$, ...) and a continuous value (in the limit $L \to \infty$) of transverse wave vector $\mathbf{k}$. These resonant subbands differ from those in a quantum well in an essential way. In a quantum well the subbands arise from truly localized states (for energies below the top of the barriers), while in a double-barrier structure the resonant subbands arise from extended states.
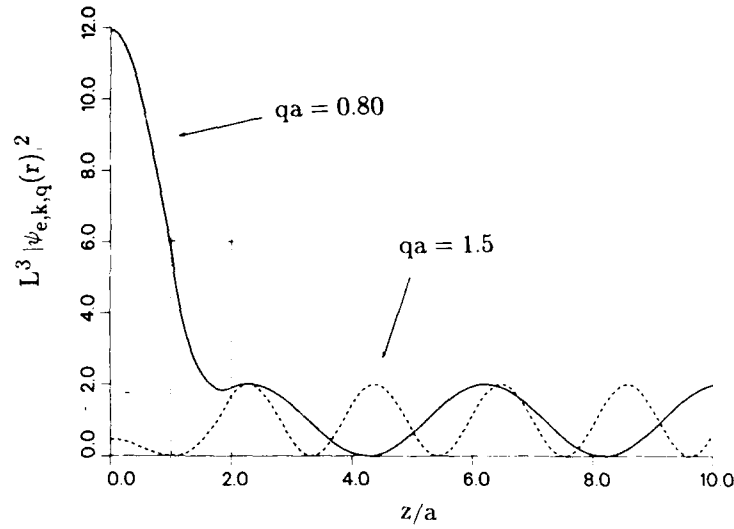

[†]See footnote on page 7.

Figure 1. Square of even function, $L^3|\psi_{e,\mathbf{k},q}(\mathbf{r})|^2$, is plotted versus spatial position z/a, for "on-resonance" $(qa = q_{e,1}a = 0.80)$, and "off-resonance" $(qa = 1.5)$, electrons for case $\mathbf{k} = 0$, $\delta = 1.0$, $\gamma = 2.0$, and $\beta = 0.73$.

3. Scattering Rate Due to One Impurity

The elastic scattering rate out of a conduction band state $|\alpha, \mathbf{k}, q\rangle$, to any other conduction band state, can be found from Fermi's golden rule

$$w_{\alpha,\mathbf{k},q} = \frac{2\pi}{\hbar} \sum_{\alpha',\mathbf{k}',q'} |\langle \alpha', \mathbf{k}', q'|U|\alpha, \mathbf{k}, q\rangle|^2 \, \delta\left(E_{\mathbf{k},q} - E_{\mathbf{k}',q'}\right), \quad (8)$$

where $U(\mathbf{r})$ is the impurity potential.[‡] For many impurity potentials the matrix element in equation (8) can be approximated as a matrix element between effective mass wave functions (see app B):

$$\langle \alpha', \mathbf{k}', q'|U|\alpha, \mathbf{k}, q\rangle = \int_\Omega d^3\mathbf{r}\, \psi^*_{\alpha',\mathbf{k}',q'}(\mathbf{r})U(\mathbf{r})\psi_{\alpha,\mathbf{k},q}(\mathbf{r}). \quad (9)$$

Calculation of this matrix element can be further simplified by substituting into equation (9) the explicit form of the wavefunction, given in equation (4), and using the Fourier expansion of the potential,

$$U(\mathbf{r}) = \sum_{\mathbf{q}} \tilde{U}(\mathbf{q})\exp(i\mathbf{q} \cdot (\mathbf{r} - \mathbf{R}_o)). \quad (10)$$

[‡]We are not considering potentials $U(\mathbf{r})$, which couple to spin degrees of freedom; hence we have omitted the spin labels on the electron states. The quantity $w_{\alpha,\mathbf{k},q}$ is the scattering rate out of a state labelled by $\alpha, \mathbf{k}, q$ with either spin up or down.

where $\mathbf{R}_o$ is the impurity position.[§] The x and y spatial integrations can then be performed, leading to a two-dimensional delta function in wave vector variables. The sum over the x- and y-wave vector components can then be done, resulting in the following expression:

$$\langle \alpha', \mathbf{k}', q' | U | \alpha, \mathbf{k}, q \rangle = \exp(-i(\mathbf{k}' - \mathbf{k}) \cdot \mathbf{R}_o) \int_{-L/2}^{+L/2} dz \, \Phi_{\alpha', \mathbf{k}', q'}^*(z) \Phi_{\alpha, \mathbf{k}, q}(z)$$

$$\cdot \sum_{p_z} \tilde{U}(\mathbf{k}' - \mathbf{k} + p_z \hat{\mathbf{z}}) \exp(i p_z (z - z_o)), \tag{11}$$

where z_o is the z-component of the impurity position vector and $\hat{\mathbf{z}}$ is a unit vector along the growth direction. The sum on p_z is over the z-component of the wave vectors appearing in equation (10), which were used to expand the impurity potential. The x- and y-components of the impurity position vector in equation (11) enter only as a phase. Because the system is translationally invariant in the x and y directions, there is no loss in generality if we choose the x and y components of the impurity position vector to be zero.

Using equation (11) we can immediately make a rough estimate of the ratio of probability for scattering of resonant electrons within the first subband, $|e, \mathbf{k}, q_{e,1}\rangle \rightarrow |e, \mathbf{k}', q'_{e,1}\rangle$, to scattering out of the first subband into the second subband, $|e, \mathbf{k}, q_{e,1}\rangle \rightarrow |o, \mathbf{k}', q_{o,1}\rangle$, by noting that the function $\Phi_{\alpha, \mathbf{k}, q}(z)$ is proportional to $F_{\alpha, \mathbf{k}}^{1/2}(qc)$. This ratio is proportional to the factor[¶]

$$\frac{F_{e, \mathbf{k}'}(q'_{e,1} a)}{F_{o, \mathbf{k}'}(q_{o,1} a)}$$

and is *independent* of the detailed form of the impurity potential. Here $q_{e,1}$ and $q'_{e,1}$ are the resonant wavevectors corresponding to transverse wave vectors $\mathbf{k}$, and $\mathbf{k}'$, respectively.[‖] For the structure used by Sollner et al [3], this ratio is $\cong 35$, for $\mathbf{k} = \mathbf{k}' = 0$.

[§] We assume that the impurity is located far from the walls of the box compared to any length scale of interest.

[¶] This result is true only for impurities located in the quantum well region. Equation (5) may suggest that at resonance the wave function is large beyond the barriers, $z > (1 + \delta)a$, because $F_{\alpha, \mathbf{k}}(qa)$ is large. This is not the case because the factor $f_\alpha(qa)$, which multiplies $F_{\alpha, \mathbf{k}}(qa)$ in the wave function, becomes small at resonance, leading to a wave function that is not large outside the quantum well region.

[‖] The resonant wave vector values $q = q_{e,1}, q_{e,2}, q = q_{e,3}, \ldots,$ and $q_{o,1}, q_{o,2}, q_{o,3}, \ldots,$ depend mildly on the corresponding value of $\mathbf{k}$. This is a consequence of the different effective masses in the quantum well and barrier regions (see eq. (6)).

In order to get a clearer picture of elastic scattering, we model a charged impurity by a spherically symmetric screened Coulomb potential [25-29]:

$$U(\mathbf{r}) = \frac{Ze^2}{\kappa} \frac{\exp(-\lambda \mid \mathbf{r} - \mathbf{R}_o \mid)}{\mid \mathbf{r} - \mathbf{R}_o \mid}, \tag{12}$$

where $1/\lambda$ is the range of the potential, Ze is the impurity charge, $\mathbf{R}_o$ is the impurity position, and κ is the static dielectric constant. For simplicity, we are neglecting the effects of anisotropic screening.[**] For this impurity potential, the sum on p_z in equation (11) can be changed to an integral and evaluated, resulting in the form

$$\langle \alpha', \mathbf{k}', q' | U | \alpha, \mathbf{k}, q \rangle = \frac{2\pi}{L^2} \frac{Ze^2}{\kappa} \frac{1}{s} \int_{-L/2}^{+L/2} dz \, \Phi^*_{\alpha', \mathbf{k}', q'}(z) \Phi_{\alpha, \mathbf{k}, q}(z) \exp(-s|z - z_o|), \tag{13}$$

where the effective screening wave vector, s, depends on the transverse momentum through the relation

$$s^2 = \lambda^2 + (\mathbf{k} - \mathbf{k}')^2. \tag{14}$$

Using equation (13), we define the dimensionless quantity $I_{\alpha', \mathbf{k}', q'; \alpha, \mathbf{k}, q}(z_o)$ by

$$\langle \alpha', \mathbf{k}', q' | U | \alpha, \mathbf{k}, q \rangle \cong \frac{4\pi \hbar^2}{m_1 a^2} \left(\frac{a}{L}\right)^3 \frac{1}{\left[\lambda^2 a_o^2 + (\mathbf{k} - \mathbf{k}')^2 a_o^2\right]^{1/2}} I_{\alpha', \mathbf{k}', q'; \alpha, \mathbf{k}, q}(z_o), \tag{15}$$

where we have introduced the Bohr radius $a_o = \kappa \hbar^2 / m_1 Ze^2$. Calculation of the function $I_{\alpha', \mathbf{k}', q'; \alpha, \mathbf{k}, q}$ is tedious but straightforward, and the results for an impurity located inside the quantum well region and inside the barrier regions are given in appendix C.

In the special case when the impurity is located inside the well, or beyond the barriers ($z_o > (1 + \delta)a$), and when s is sufficiently large i.e., $|\mathbf{k} - \mathbf{k}'| a$ is large (but still $(\mathbf{k} - \mathbf{k}') \cdot \mathbf{c} \ll 1$, where $\mathbf{c}$ is a primitive lattice vector) the matrix element can be approximated by

$$\langle \alpha', \mathbf{k}', q' | U | \alpha, \mathbf{k}, q \rangle = \frac{8\pi}{L^3} \frac{Ze^2}{\kappa} \frac{\left\{ F_{\alpha', \mathbf{k}'}(q'a) F_{\alpha, \mathbf{k}}(qa) \right\}^{1/2}}{\lambda^2 + (\mathbf{k} - \mathbf{k}')^2} \Phi^*_{\alpha', \mathbf{k}', q'}(z_o) \Phi_{\alpha, \mathbf{k}, q}(z_o), \tag{16}$$

where we have assumed $sL \gg 1$, dropping terms of order $\exp(-sL/2)$. This result shows that the matrix element is large at resonant values of initial and final electron wave vectors, where $F_{\alpha', \mathbf{k}'}(q'a)$ and $F_{\alpha, \mathbf{k}}(qa)$

[**]A correct treatment of screening in a double-barrier structure is a difficult problem in itself. We have chosen to model the impurity by a physically plausible zeroth-order potential with as few unknown parameters as possible. Introducing anisotropic screening would undoubtedly introduce more unknown parameters.

11

¹ ₋ve peaks. As $|\mathbf{k} - \mathbf{k}'|$ increases, the magnitude of the matrix element decreases. This is a consequence of the rapid oscillations in the transverse part of the wave function that serve to diminish the integral.

We now substitute the explicit form of the matrix element given in equation (15) into equation (8) for the scattering rate and sum over all final states. In the limit $L \to \infty$, the density of wave vectors approaches $(L/2\pi)^3$ per unit volume in $(\mathbf{k}, q)$-space, and we can change the sum over wave vectors to an integral over the region $q' > 0$ and $-\infty < k'_x, k'_y < +\infty$. In cylindrical coordinates, we do the q integration, leading to the following expression for the scattering rate:

$$w_{\alpha,\mathbf{k},q} = \frac{8\hbar}{m_1 a_o^2} \left(\frac{a}{L}\right)^3 S_{\alpha,\mathbf{k},q}(z_o),\tag{17}$$

where

$$S_{\alpha,\mathbf{k},q}(z_o) = \int_0^{[\check{k}^2 + \check{q}^2]^{1/2}} d\check{k}' \, \check{k}' \int_0^{+1} dx \frac{1}{\sqrt{1 - x^2}} \frac{1}{[\check{k}^2 + \check{q}^2 - \check{k}'^2]^{1/2}}$$

$$\cdot \sum_{\alpha'=e,o} \left[G(\alpha', \check{k}', \check{q}; \alpha, \check{k}, q; x) + G(\alpha', \check{k}', \check{q}; \alpha, \check{k}, q; -x) \right].\tag{18}$$

In equation (18) we have introduced the dimensionless function

$$G(\alpha', \check{k}', \check{q}'; \alpha, \check{k}, \check{q}; x) = \frac{1}{\lambda^2 a^2 + (\mathbf{k} - \mathbf{k}')^2 a^2} \left| I_{\alpha',\mathbf{k}',q';\alpha,\mathbf{k},q}(z_o) \right|^2,\tag{19}$$

and the dimensionless wave vectors $\check{k} = |\mathbf{k}|a$, $\check{k}' = |\mathbf{k}'|a$, $\check{q} = qa$. In the integrand of equation (18), the functions G are evaluated at $\check{q}' = \check{q}$, where $\check{q} = [\check{k}^2 + \check{q}^2 - \check{k}'^2]^{1/2}$. The integration is over the dimensionless final transverse wave vector, $\check{k}'$, and $x = \cos(\phi)$, where ϕ is the angle between the initial and final wave vectors, $\mathbf{k}$ and $\mathbf{k}'$. The integration over $\check{k}'$ has a finite upper limit, a consequence of energy conservation. The double integral in equation (18) was done numerically, and the results are shown in figures 2 and 3, for parameters characterizing the structure used by Sollner et al [3], for an impurity potential range $1/\lambda = 10a$.

The solid curve in figure 2 is the scattering rate out of an even state. The peak at $qa = 0.898$ (off the scale) is due to the lowest energy even resonance, while the peak near $qa = 2.0$ is due to the next higher energy even resonance. The dashed line shows the scattering rate out of odd states, and the peak at $qa = 1.66$ is due to the lowest energy odd resonance. As one would expect, the peaks in the even and odd scattering rates alternate with increasing wave vector. For this structure and

12

potential range, the ratio of the scattering rate at the largest even peak to the largest odd peak is approximately 100. The dotted line in figure 2 shows the scattering rate out of even states in a bulk semiconductor (where $\gamma = 0$ and $\beta = 1$) with the same range potential $1/\lambda = 10a$. The large scattering rate near $q = 0$ is due to the Coulombic nature of the impurity potential (there would be a divergence for $1/\lambda \to \infty$). Electrons which occupy states near the lowest energy resonance experience scatterings 3000 times more frequently than occurs in the bulk. For a longer range potential, the peaks in the scattering rate would be less pronounced. However, the overall scattering rate would be bigger because of increased wave function and impurity potential overlap. Because of the large scattering rates for states near resonance, we expect that the local density of states, averaged over the quantum well region, can be significantly modified from that calculated without impurities [15,17].
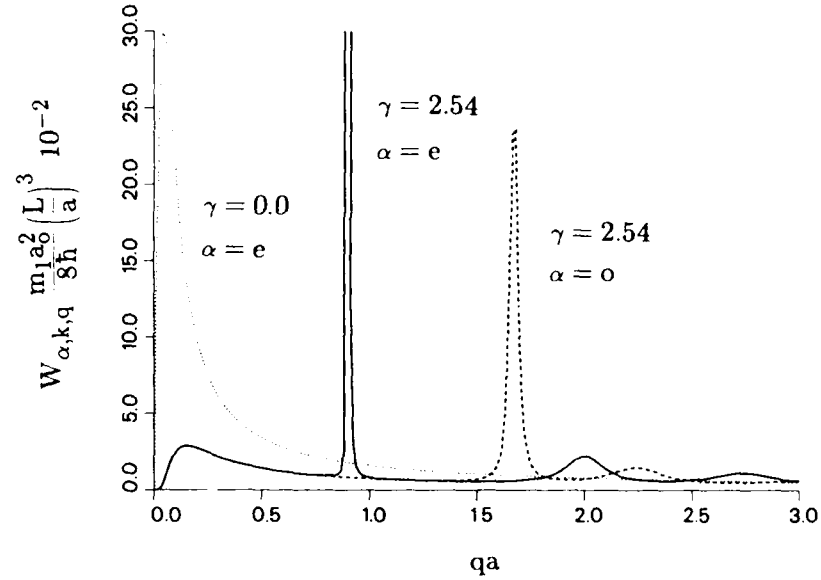

Figure 2. Dimensionless scattering rate, $w_{\alpha,k,q}(m_1 a_o^2 L^3)/(8\hbar a^3)$, is plotted versus qa, for an impurity located at center of quantum well, $z_o = 0$. Solid and dashed curves are scattering rates out of even and odd states, $\alpha = e$ and $\alpha = o$, respectively, for $k = 0$ and barrier height $V_o = 0.23$ eV, effective mass in quantum well $m_1 = 0.067$, $\delta = 2.0$, $\beta = 0.73$, and impurity potential range $1/\lambda = 10a$. For case $\alpha = e$, peak at $qa = 0.898$ is off the scale, reaching a maximum value of ~ 3000, in units on graph. Dotted curve is scattering rate in absence of a double-barrier structure, $\gamma = 0.0$, $\beta = 1.0$, for a potential range $1/\lambda = 10a$.

13

Figure 3. Solid line is a plot of dimensionless scattering rate, $w_{e,\mathbf{k},q}(m_1 a_o^2 L^3)/(8\hbar a^3)$, versus impurity position z_o/a, for resonant state $\mathbf{k} = 0$, $qa = q_{e,1}a = 0.897$, for same structure as in figure 2. Dashed line below solid curve shows position of barrier.
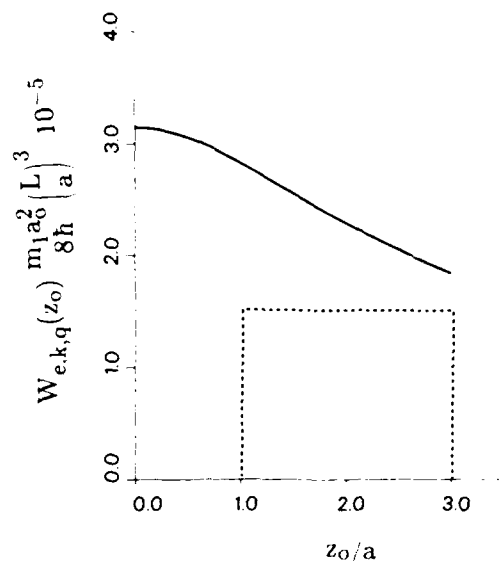
Figure 3 shows a plot of the scattering rate as a function of impurity position for states in the range of the lowest energy even resonance. Impurities near the center of the quantum well give a somewhat larger rate of scattering than those near the edges, because of the peaked nature of the even wave functions. However, for this potential range, this is a minor effect. In the calculations above, we made a somewhat arbitrary choice of the potential range: $1/\lambda = 10a$. For a shorter range potential, the dependence of the scattering rate on impurity position would be stronger than that shown in figure 3; however, the overall values of the scattering rates would be smaller because of decreased overlap of the impurity potential with the electron wave functions.

4. Random Distribution of Impurities

The total scattering rate, $W_{\alpha,\mathbf{k},q}$, due to a macroscopic number of randomly distributed impurities can be found from the one impurity scattering rate in equation (17) by summing over impurity position vectors $\mathbf{R}_o$. This can be seen by considering the matrix element of the total potential, U_{N_i}, which is a sum of N_i one-impurity potentials, each centered about a position vector $\mathbf{R}_o$ from a set of N_i random position[††]

[††]If the impurities are substitutional then these vectors coincide with crystal lattice sites.

14

vectors, $\{\mathbf{R}_o\}$. The matrix element for scattering from N_i impurities is then a sum of single impurity matrix elements, each given by equation (11), and can be written as

$$\langle \alpha', \mathbf{k}', q' | U_{N_i} | \alpha, \mathbf{k}, q \rangle = \sum_{\{\mathbf{R}_o\}} \exp(-i\mathbf{K} \cdot \mathbf{R}_o) A_{p,p'}(z_o). \qquad (20)$$

where we have introduced the shorthand notation $\mathbf{K} = \mathbf{k}' - \mathbf{k}$, $p = \{\alpha, \mathbf{k}, q\}$ and $p' = \{\alpha', \mathbf{k}', q'\}$. The absolute square of this matrix element can then be written as

$$|\langle \alpha', \mathbf{k}', q' | U_{N_i} | \alpha, \mathbf{k}, q \rangle|^2 = \sum_{\{\mathbf{R}_o\}} \sum_{\{\mathbf{R}_o'\}} \exp(-i\mathbf{K}\cdot(\mathbf{R}_o - \mathbf{R}_o')) A_{p,p'}(z_o) A_{p,p'}^*(z_o').$$

For a macroscopic number of impurities at random positions, the phases in the sum above add incoherently, resulting in a sum that is close to zero except when $\mathbf{R}_o = \mathbf{R}_o'$ or $\mathbf{K} = 0$. These two conditions lead to two terms,

$$|\langle \alpha', \mathbf{k}', q' | U_{N_i} | \alpha, \mathbf{k}, q \rangle|^2 = \sum_{\{\mathbf{R}_o\}} |A_{p,p'}(z_o)|^2 \quad + \quad |\sum_{\{\mathbf{R}_o\}} A_{p,p'}(z_o)|^2 \, \delta_{\mathbf{k},\mathbf{k}'}, \qquad (21)$$

respectively, where the sums are over the z_o-components of the set of random impurity positions. The second term is negligibly small because the random phases cancel in the summation over z_o. Substitution of the first term into Fermi's golden rule yields a total scattering rate which is a sum of single impurity scattering rates, given in equation (17).

In a bulk semiconductor the single impurity scattering rate $w_{\alpha,\mathbf{k},q}(z_o)$ is roughly independent of position z_o, leading to a total scattering rate proportional to impurity density $n_i = N_i/L^3$. However, in a double-barrier structure the function $S_{\alpha,\mathbf{k},q}(z_o)$ can have a strong spatial dependence in the quantum well region because of the presence of the resonances. For on-resonance (off-resonance) electrons the wave function amplitude in the quantum well region is large (small) compared to outside this region, leading to a large (small) contribution to the total scattering rate from impurities in the quantum well.

The sum of equation (17) over impurity positions z_o can be approximated by the factor n_i times an integral over the crystal volume. Integration over the x_o, y_o coordinates contributes a factor L^2, resulting in a total scattering rate that can be written as

$$W_{\alpha,\mathbf{k},q} = \frac{8\hbar}{m_1 a_o^2} n_i a^3 \left[\frac{a}{L} \int_{R_1} S_{\alpha,\mathbf{k},q}(z_o) d(z_o/a) + \frac{a}{L} \int_{R_2} S_{\alpha,\mathbf{k},q}(z_o) d(z_o/a) \right], \qquad (22)$$

15

where the integration region R_1 is the well plus barrier, $|z_o/a| < 1 + \delta$, and R_2 is the region outside the barriers, $1 + \delta < |z_o/a| < L/2a$.

The first term in equation (22) gives the contribution to the total scattering rate from the quantum well (and barriers) region, and the second term gives the contribution from the rest of the crystal. Since the quantum well forms a negligible volume fraction of the whole crystal volume, it may appear at first sight that the first term is $O(a/L)$ times the second term, and hence is completely negligible. This is true for electrons that are in states away from the resonance regions. However, electrons with wave vectors that satisfy the resonance conditions (see sect. 1) may have a macroscopic fraction (i.e., not $O(a/L)$) of their normalization in the quantum well region.[‡‡] For resonant electrons, this leads to a situation where the contribution to the total scattering rate from impurities in the quantum well region, given by the first term in equation (22), is comparable to the contribution from the rest of the crystal, given by the second term. This is essentially a finite size effect. As expected, for sufficiently large crystals, $L \to \infty$, the second term always becomes larger. We find that for a sample whose total thickness is 30 μ, with 40-Å well and barriers, and an impurity potential range $1/\lambda = 10a$, the first term is comparable to the second.

5. Conclusion

Within the framework of a simple model, we explored elastic impurity scattering for electrons in resonant states. We found that for certain parameters, such as screening length and well and barrier widths, impurities in the quantum well region can contribute significantly and even dominate the scattering rate, despite the fact that a quantum well occupies a negligible volume fraction of the crystal. We have used a simple model of isotropic screening which is an oversimplification. Proper treatment of screening in a double-barrier structure is in itself a difficult problem. We have also ignored effects associated with space charge, external electric field, and band nonparabolicity.

Acknowledgments

[‡‡]The extreme case where all electron probability is localized is in the case of a sufficiently large quantum well, where a true bound state with unity normalization appears.

16

References

1. See, for instance, *Synthetic Modulated Structures*, edited by L. L. Chang and B. C. Giessen, Academic Press, New York (1985). For a more recent review see IEEE J. Quantum Electron. QE-22 (1986), 9.

2. L. L. Chang, L. Esaki, and R. Tsu, Appl. Phys. Lett. 24 (1974), 593.

3. T.C.L.G. Sollner, W. D. Goodhue, P. E. Tannenwald, C. D. Parker, and D. D. Peck, Appl. Phys. Lett. 43 (1983), 588.

4. T.C.L.G. Sollner, P. E. Tannenwald, D. D. Peck, and W. D. Goodhue, Appl. Phys. Lett. 45 (1984), 1319.

5. A. R. Bonnefoi, R. T. Collins, T. C. McGill, R. D. Burnham, and F. A. Ponce, Appl. Phys. Lett. 46 (1985), 285.

6. E. E. Mendez, W. I. Wang, B. Ricco, and L. Esaki, Appl. Phys. Lett. 47 (1985), 415.

7. J. Söderström, T. G. Andersson, and J. Westin, Superlattices and Microstructures 3 (1987), 283.

8. M. A. Reed and J. W. Lee, Appl. Phys. Lett. 50 (1987), 845.

9. E. E. Mendez, W. I. Wang, E. Calleja, and C.E.T. Goncalves da Silva, Appl. Phys. Lett. 50 (1987), 1263.

10. V. J. Goldman, D. C. Tsui, and J. E. Cunningham, Phys. Rev. B 35 (1987), 9387.

11. V. J. Goldman, D. C. Tsui, and J. E. Cunningham, Phys. Rev. Lett. 58 (1987), 1256.

12. M. Tsuchiya, T. Matsusue, and H. Sakaki, Phys. Rev. Lett. 59 (1987), 2356.

13. E. Wolak, K. L. Lear, P. M. Pitner, E. S. Hellman, B. G. Park, T. Weil, and J. S. Harris, Jr., Appl. Phys. Lett. 53 (1988), 201.

14. R. Tsu and L. Esaki, Appl. Phys. Lett. 22 (1973), 562.

15. T. B. Bahder, J. D. Bruno, R. G. Hay, and C. A. Morrison, Phys. Rev. B 37 (1988), 6256.

16. J. D. Bruno, T. B. Bahder, and C. A. Morrison, Phys. Rev. B 37 (1988), 7098.

17. J. D. Bruno and T. B. Bahder, Phys. Rev. B 39 (1989), 3659.

18. M. Büttiker, IBM J. Res. Develop. 32 (1988), 63.

19. V. N. Ermakov and E. A. Ponezha, Phys. Stat. Sol. (b) 145 (1988), 545.

20. B. Ricco and P. Olivo, Superlattices and Microstructures 2 (1986), 79.

21. H. Ohnishi, T. Inata, S. Muto, N. Yokoyama, and A. Shibatomi, Appl. Phys. Lett. 49 (1986), 1248.

22. A. D. Stone and P. A. Lee, Phys. Rev. Lett. 54 (1985), 1196.

23. See for example, B. R. Nag, *Electron Transport in Compound Semiconductors*, Springer-Verlag, N. Y. (1980).

24. J. M. Luttinger and W. Kohn, Phys. Rev. 97 (1955), 869.

25. L. M. Falicov and M. Cuevas, Phys. Rev. 164 (1967), 1025.

26. J. B. Krieger and S. Strauss, Phys. Rev. 169 (1968), 674.

27. D. Long, Phys. Rev. 176 (1968), 923.

28. D. L. Rode and S. Knight, Phys. Rev. B 3 (1971), 2534.

29. H. I. Ralph, G. Simpson, and R. J. Elliott, Phys. Rev. B 11 (1975), 2948.

Appendix A. Functions in Equation (5)

The functions in equation (5) in the main body of the text are defined below:

$$d_\alpha(u) = \frac{1}{2}\exp(-w(u))\eta_\alpha(u)$$

$$e_\alpha(u) = \frac{1}{2}\exp(w(u))\xi_\alpha(u)$$

$$f_\alpha(u) = \frac{1}{4}\exp(-i(1+\delta)u)\left\{\exp(w(u)\delta)\left(1+\frac{\beta w(u)}{iu}\right)\eta_\alpha(u) + \exp(-w(u)\delta)\left(1-\frac{\beta w(u)}{iu}\right)\xi_\alpha(u)\right\}$$

$$g_\alpha(u) = \frac{1}{4}\exp(i(1+\delta)u)\left\{\exp(w(u)\delta)\left(1-\frac{\beta w(u)}{iu}\right)\eta_\alpha(u) + \exp(-w(u)\delta)\left(1+\frac{\beta w(u)}{iu}\right)\xi_\alpha(u)\right\}$$

$$\eta_e(u) = \cos(u) - \frac{u}{\beta w(u)}\sin(u)$$

$$\eta_o(u) = \sin(u) + \frac{u}{\beta w(u)}\cos(u)$$

$$\xi_e(u) = \cos(u) + \frac{u}{\beta w(u)}\sin(u)$$

$$\xi_o(u) = \sin(u) - \frac{u}{\beta w(u)}\cos(u).$$

The function $F_{\alpha,\mathbf{k}}(u)$ in equation (5), correct to zeroth order in a/L, can be written as

$$F_{\alpha,\mathbf{k}}(u) = \frac{u^2}{D_\alpha(u)}.$$

For $\alpha = e$, the function $D_e(u)$, in the denominator is given by

$$D_e(u) = u^2 + \frac{1}{2}\left(\beta\tilde{\gamma} + (1-\beta)u^2\right)\left(\cos^2(u) + \frac{u^2}{\beta(\tilde{\gamma}-u^2)}\sin^2(u)\right)\left(\cosh\left(2\delta w(u)\right) - 1\right)$$

$$-\frac{1}{2\beta w(u)}\left(\beta\tilde{\gamma} + (1-\beta)u^2\right)u\sin(2u)\sinh\left(2\delta w(u)\right).$$

For $\alpha = o$, the function $D_o(u)$ can be obtained from $D_e(u)$ by the replacements $\sin(u) \to \cos(u)$, $\cos(u) \to -\sin(u)$, and $\sin(2u) \to -\sin(2u)$.

19

Appendix B.   Impurity Matrix Elements

For many interesting impurity potentials the matrix element in equation (8) (see main body of text) can be expressed as a matrix element between envelope functions. This can be shown by changing the integration over all space to a sum over all lattice vectors $\mathbf{R}$ and an integral over a single primitive cell of volume v:

$$\langle \alpha', \mathbf{k}', q' | U | \alpha, \mathbf{k}, q \rangle = \sum_{\mathbf{R}} \int_v d^3 r \, \psi^*_{\alpha', \mathbf{k}', q'}(\mathbf{r} + \mathbf{R}) u^*_c(\mathbf{r} + \mathbf{R}) U(\mathbf{r} + \mathbf{R}) \psi_{\alpha, \mathbf{k}, q}(\mathbf{r} + \mathbf{R}) u_c(\mathbf{r} + \mathbf{R}). \quad (B-1)$$

The envelope functions vary slowly over a primitive cell, so they can be expanded about an arbitrary lattice vector, $\psi_{\alpha, \mathbf{k}, q}(\mathbf{R} + \mathbf{r}) = \psi_{\alpha, \mathbf{k}, q}(\mathbf{R}) + \nabla \psi_{\alpha, \mathbf{k}, q}(\mathbf{R}) \cdot \mathbf{r} + \cdots$, while the Bloch functions are periodic, $u_c(\mathbf{r} + \mathbf{R}) = u_c(\mathbf{r})$. Using this in equation (B-1) and keeping only the first term, we have

$$\langle \alpha', \mathbf{k}', q' | U | \alpha, \mathbf{k}, q \rangle = \sum_{\mathbf{R}} \int_v d^3 r \, |u_c(\mathbf{r})|^2 U(\mathbf{r} + \mathbf{R}) \psi^*_{\alpha', \mathbf{k}', q'}(\mathbf{R}) \psi_{\alpha, \mathbf{k}, q}(\mathbf{R}). \quad (B-2)$$

We now Fourier expand the impurity potential in plane waves as in equation (10) of the text. In this expansion $\mathbf{q}$ takes the values $(n_x, n_y, n_z) 2\pi / L$, where n_x, n_y, n_z, are integers. Using this expansion in equation (B-2) we get

$$\langle \alpha', \mathbf{k}', q' | U | \alpha, \mathbf{k}, q \rangle = \sum_{\mathbf{q}} \tilde{U}(\mathbf{q}) \sum_{\mathbf{R}} \exp(i \mathbf{q} \cdot (\mathbf{R} - \mathbf{R}_o)) \psi^*_{\alpha', \mathbf{k}', q'}(\mathbf{R}) \psi_{\alpha, \mathbf{k}, q}(\mathbf{R}) \int_v d^3 r \, |u_c(\mathbf{r})|^2 \exp(i \mathbf{q} \cdot \mathbf{r}).$$
$$(B-3)$$

If we assume that $\tilde{U}(\mathbf{q}) \approx 0$ for $|\mathbf{q}| > q_c$, where q_c is some cutoff wave vector that satisfies $q_c \ll 1/|\mathbf{c}|$, and $\mathbf{c}$ is a primitive lattice vector, we can cut off the sum on $\mathbf{q}$, in equation (B-3), at $|\mathbf{q}| = q_c$. For all $\mathbf{r}$ within a cell we have $\mathbf{q} \cdot \mathbf{r} \ll 1$, so we can expand the exponential in equation (B-3), keeping only the first term, and write

$$\int_v d^3 r \, |u_c(\mathbf{r})|^2 \exp(i \mathbf{q} \cdot \mathbf{r}) = v + O(q_c |\mathbf{R}|),$$

where we are assuming that the Bloch functions are normalized to v over the primitive cell. Using these approximations in equation

21

(B-3), changing the sum on $\mathbf{R}$ to an integral over the crystal volume Ω,

$$v \sum_{\mathbf{R}} \rightarrow \int_{\Omega} d^3 \mathbf{R}, \qquad (B-5)$$

we can write the matrix element in equation (B-3) approximately as given in equation (9) of the text. Note that a delta-function impurity potential does not allow this simplification.

Appendix C.   Definition of the Function $I_{\alpha',\mathbf{k}',q';\alpha,\mathbf{k},q}$

In this appendix we give the explicit form of the quantity $I_{\alpha',\mathbf{k}',q';\alpha,\mathbf{k},q}(z_o)$, introduced in equation (15) of the text. When the impurity is inside the quantum well region, $0 \leq z_o \leq a$,

$$I_{\alpha',\mathbf{k}',q';\alpha,\mathbf{k},q}(z_o) = \frac{1}{4} \frac{1}{[D_{\alpha'}(q'a)D_\alpha(qa)]^{1/2}} \left\{ (i)^{\alpha+\alpha'} a\, q\, q'\, \hat{R}_{\alpha+\alpha'} \left[\exp(-sz_o) \frac{\exp(-s+i(q+q'))-1}{-s+i(q+q')} \right. \right.$$

$$+ (-1)^{\alpha'} \exp(-sz_o) \frac{\exp(-s+i(q-q'))-1}{-s+i(q-q')}$$

$$+ (-1)^{\alpha+\alpha'} \exp(sz_o) \frac{\exp(-s+i(q+q')) - \exp[(-s+i(q+q'))z_o]}{-s+i(q+q')}$$

$$+ (-1)^{\alpha} \exp(sz_o) \frac{\exp(-s+i(q-q')) - \exp[(-s+i(q-q'))z_o]}{-s+i(q-q')}$$

$$- (-1)^{\alpha+\alpha'} \exp(-sz_o) \frac{1 - \exp[(s+i(q+q'))z_o]}{s+i(q+q')}$$

$$\left. - (-1)^{\alpha} \exp(-sz_o) \frac{1 - \exp[(s+i(q-q'))z_o]}{s+i(q-q')} \right]$$

$$+ \frac{1}{a} [\exp(s(z_o-1)) + (-1)^{\alpha+\alpha'} \exp(-s(z_o+1))] \left[\tilde{\eta}^*_{\alpha'}(q'a)\,\tilde{\eta}_\alpha(qa) \frac{\exp[(-s+\lambda+\lambda'^*)\delta a]-1}{-s+\lambda+\lambda'^*} \right.$$

$$+ \tilde{\xi}^*_{\alpha'}(q'a)\,\tilde{\eta}_\alpha(qa) \frac{\exp[(-s+\lambda-\lambda'^*)\delta a]-1}{-s+\lambda-\lambda'^*}$$

$$+ \tilde{\eta}^*_{\alpha'}(q'a)\,\tilde{\xi}_\alpha(qa) \frac{\exp[(-s-\lambda+\lambda'^*)\delta a]-1}{-s-\lambda+\lambda'^*} + \tilde{\xi}^*_{\alpha'}(q'a)\,\tilde{\xi}_\alpha(qa) \frac{\exp[(-s-\lambda-\lambda'^*)\delta a]-1}{-s-\lambda-\lambda'^*}$$

$$+ \tilde{f}^*_{\alpha'}(q'a)\,\tilde{f}_\alpha(qa) \frac{\exp(-s\delta a)}{s-i(q-q')} + \tilde{g}^*_{\alpha'}(q'a)\,\tilde{f}_\alpha(qa) \frac{\exp(-s\delta a)}{s-i(q+q')}$$

$$\left. \left. + \tilde{f}^*_{\alpha'}(q'a)\,\tilde{g}_\alpha(qa) \frac{\exp(-s\delta a)}{s+i(q+q')} + \tilde{g}^*_{\alpha'}(q'a)\,\tilde{g}_\alpha(qa) \frac{\exp(-s\delta a)}{s+i(q-q')} \right] \right\}. \tag{C-1}$$

When the impurity is inside the barrier region, $a \leq z_o \leq (1+\delta)a$,

$$I_{\alpha',\mathbf{k}',q';\alpha,\mathbf{k},q}(z_o) = \frac{1}{4} \frac{1}{[D_{\alpha'}(q'a)D_{\alpha}(qa)]^{1/2}} \left\{ (i)^{\alpha+\alpha'} a\, q\, q'\, \exp(-sz_o) \dot{R}_{\alpha+\alpha'} \left[\frac{\exp(-s+i(q+q'))-1}{-s+i(q+q')} \right.\right.$$

$$+ (-1)^{\alpha'} \frac{\exp(-s+i(q-q'))-1}{-s+i(q-q')}$$

$$+ (-1)^{\alpha+\alpha'} \exp(-sz_o) \frac{\exp(s+i(q+q'))-1}{s+i(q+q')}$$

$$\left. + (-1)^{\alpha} \frac{\exp(s+i(q-q'))-1}{s+i(q-q')} \right]$$

$$.+ \frac{1}{a}(-1)^{\alpha+\alpha'} \exp(-s(z_o+1)) \left[\check{\eta}_{\alpha'}^*(q'a)\,\check{\eta}_{\alpha}(qa) \frac{\exp[(-s+\lambda+\lambda'^*)a\delta]-1}{-s+\lambda+\lambda'^*} \right.$$

$$+ \check{\xi}_{\alpha'}^*(q'a)\,\check{\eta}_{\alpha}(qa) \frac{\exp[(-s+\lambda-\lambda'^*)a\delta]-1}{-s+\lambda-\lambda'^*}$$

$$+ \check{\eta}_{\alpha'}^*(q'a)\,\check{\xi}_{\alpha}(qa) \frac{\exp[(-s-\lambda+\lambda'^*)a\delta]-1}{-s-\lambda+\lambda'^*}$$

$$\left. + \check{\xi}_{\alpha'}^*(q'a)\,\check{\xi}_{\alpha}(qa) \frac{\exp[(-s-\lambda-\lambda'^*)a\delta]-1}{-s-\lambda-\lambda'^*} \right]$$

$$+ \frac{1}{a} \exp(-s(z_o-1)) \left[\check{\eta}_{\alpha'}^*(q'a)\,\check{\eta}_{\alpha}(qa) \frac{\exp[(s+\lambda+\lambda'^*)(z_o-1)]-1}{s+\lambda+\lambda'^*} \right.$$

$$+ \check{\xi}_{\alpha'}^*(q'a)\,\check{\eta}_{\alpha}(qa) \frac{\exp[(s+\lambda-\lambda'^*)(z_c-1)]-1}{s+\lambda-\lambda'^*}$$

$$+ \check{\eta}_{\alpha'}^*(q'a)\,\check{\xi}_{\alpha}(qa) \frac{\exp[(s-\lambda+\lambda'^*)(z_o-1)]-1}{s-\lambda+\lambda'^*}$$

$$\left. + \check{\xi}_{\alpha'}^*(q'a)\,\check{\xi}_{\alpha}(qa) \frac{\exp[(s-\lambda-\lambda'^*)(z_o-1)]-1}{s-\lambda-\lambda'^*} \right]$$

$$+ \; \frac{1}{a} \; \exp(s(z_o - 1)) \Big[\check{\eta}^*_{\alpha'}(q'a) \, \check{\eta}_{\alpha}(qa) \frac{\exp[(-s + \lambda + \lambda'^*)a\delta] - \exp[(-s + \lambda + \lambda'^*)(z_o - 1)]}{-s + \lambda + \lambda'^*}$$

$$+ \; \check{\xi}^*_{\alpha'}(q'a) \, \check{\eta}_{\alpha}(qa) \frac{\exp[(-s + \lambda - \lambda'^*)a\delta] - \exp[(-s + \lambda - \lambda'^*)(z_o - 1)]}{-s + \lambda - \lambda'^*}$$

$$+ \; \check{\eta}^*_{\alpha'}(q'a) \, \check{\xi}_{\alpha}(qa) \frac{\exp[(-s - \lambda + \lambda'^*)a\delta] - \exp[(-s - \lambda + \lambda'^*)(z_o - 1)]}{-s - \lambda + \lambda'^*}$$

$$+ \; \check{\xi}^*_{\alpha'}(q'a) \, \check{\xi}_{\alpha}(qa) \frac{\exp[(-s - \lambda - \lambda'^*)a\delta] - \exp[(-s - \lambda - \lambda'^*)(z_o - 1)]}{-s - \lambda - \lambda'^*} \Big]$$

$$- \; \frac{1}{a} \; \exp(-sa(1 + \delta)) \Big(\exp(sz_o) + (-1)^{\alpha + \alpha'} \exp(-sz_o) \Big) \Big[\frac{\check{f}^*_{\alpha'}(q'a) \, \check{f}_{\alpha}(qa)}{-s + i(q - q')}$$

$$+ \; \frac{\check{g}^*_{\alpha'}(q'a) \, \check{f}_{\alpha}(qa)}{-s + i(q + q')} + \frac{\check{f}^*_{\alpha'}(q'a) \, \check{g}_{\alpha}(qa)}{-s - i(q + q')} + \frac{\check{g}^*_{\alpha'}(q'a) \, \check{g}_{\alpha}(qa)}{-s - i(q - q')} \Big] \Big\}. \qquad (C-2)$$

In equations (C-1) and (C-2) we have introduced the functions

$$\check{\eta}_{\alpha}(qa) = qa \, \eta_{\alpha}(qa),$$

$$\check{\xi}_{\alpha}(qa) = qa \, \xi_{\alpha}(qa),$$

$$\check{f}_{\alpha}(qa) = 2qa \, \exp[iqa(\delta + 1)] f_{\alpha}(qa),$$

$$\check{g}_{\alpha}(qa) = 2qa \, \exp[-iqa(\delta + 1)] g_{\alpha}(qa),$$

$$\lambda = \frac{1}{a} w(qa),$$

where $\eta_{\alpha}(qa)$, $\xi_{\alpha}(qa)$, $f_{\alpha}(qa)$, $g_{\alpha}(qa)$, and $w(u)$ are defined in appendix A and equation (6), respectively. When these functions appear with primed subscripts, the final state value of the transverse wave vector ($= \mathbf{k}'$) should be used in their definition. The parameter λ', for the final state, is defined by $\lambda' = w(q'a)/a$, where $\mathbf{k}'$ is used in equation (7) in place of $\mathbf{k}$. We have also introduced the operator $\hat{R}_{\alpha}$, which operates on a complex number z according to the definition $\hat{R}_{\alpha} z = z + (-1)^{\alpha} z^*$, where α is an integer. In equations (C-1) and (C-2) we use the convention that $\alpha = 0$ for an even state and $\alpha = 1$ for an odd state.

25

DISTRIBUTION

ADMINISTRATOR
DEFENSE TECHNICAL INFORMATION CENTER
ATTN DTIC-DDA (12 COPIES)
CAMERON STATION, BUILDING 5
ALEXANDRIA, VA 22304-6145

ENGINEERING SOCIETIES LIBRARY
ATTN ACQUISITIONS DEPT
345 EAST 47TH STREET
NEW YORK, NY 10017

COMMANDER
US ARMY MATERIALS & MECHANICS
  RESEARCH CENTER
ATTN DRXMR-TL, TECH LIBRARY BR
WATERTOWN, MA 02172

COMMANDER
US ARMY RESEARCH OFFICE (DURHAM)
PO BOX 12211
ATTN B. D. GUENTHER
ATTN R. J. LONTZ
ATTN C. BOGOSIAN
ATTN M. STROSCIO
RESEARCH TRIANGLE PARK, NC 27709

COMMANDER
US ARMY COMBAT SURVEILLANCE & TARGET
  ACQUISITION LABORATORY
ATTN G. IAFRATE
ATTN R. LAREAU
ATTN D. SMITH
ATTN L. YERKE
ATTN T. AUCOIN
FT MONMOUTH, NJ 07703

THE AEROSPACE CORPORATION
ATTN FRANK VERNON
ATTN RICHARD KRANTZ
P.O. BOX 92957
LOS ANGELES, CA 90009

AT&T BELL LABORATORIES
ATTN B. A. WILSON
ATTN A. Y. CHO
ATTN S. LURYI
ATTN J. E. CUNNINGHAM
ATTN W. T. TSANG
600 MOUNTAIN AVE
MURRAY HILL, NJ 07974

BERKELEY RESEARCH ASSOCIATES, INC
PO BOX 852
ATTN R. D. TAYLOR
SPRINGFIELD, VA 22150

DIRECTOR
ADVISORY GROUP ON ELECTRON DEVICES
ATTN SECTRY, WORKING GROUP D
201 VARICK STREET
NEW YORK, NY 10013

HONEYWELL PHYSICAL SCIENCES CTR
ATTN P. P. RUDIN
10701 LYNDALE AVENUE SOUTH
BLOOMINGTON, MN 55420

IBM
T. J. WATSON RESEARCH CENTER
ATTN P. J. PRICE
ATTN L. L. CHANG
ATTN L. ESAKI
ATTN E. E. MENDEZ
ATTN M. B'TTIKER
YORKTOWN HEIGHTS, NY 10598

LINCOLN LABORATORIES
ATTN E. R. BROWN
ATTN T. C. L. G. SOLLNER
ATTN W. D. GOODHUE
ATTN C. D. PARKER
MASSACHUSETTS INSTITUTE OF
  TECHNOLOGY
LEXINGTON, MA 02173

MARTIN MARIETTA
ATTN F. CROWNE
ATTN J. LITTLE
ATTN T. WORCHESKY
1450 SOUTH ROLLING ROAD
BALTIMORE, MD 21226

SCIENTIFIC APPLICATIONS, INC.
ATTN B. GORDON
3 DOWNING RD
HANOVER, NH 03755

TEXAS INSTRUMENTS
ATTN W. R. FRENSLEY

TEXAS INSTRUMENTS (cont'd)
ATTN M.A. REED
ATTN J. W. LEE
ATTN H-L. TSAI
CENTRAL RESEARCH LABORATORY
DALLAS, TX 76265

XEROX CORPORATION
ATTN R. D. BURNHAM
ATTN F. A. PONCE
PALO ALTO, CA 94304

CALIFORNIA INSTITUTE OF
    TECHNOLOGY
ATTN A. R. BONNEFOI
ATTN T. C. McGILL
PASADENA, CA 91125

UNIVERSITY OF CALIFORNIA
    LOS ANGELES
ATTN B. JOGAI
ATTN K. L. WANG
DEPT. OF ELEC. ENG.
LOS ANGELES, CA 90024

UNIVERSITY OF HAWAII
DEPT OF PHYSICS
ATTN C. VAUSE
2505 CORREA RD
HONOLULU, HI 96822

NORTH CAROLINA STATE
    UNIVERSITY
ATTN G. S. LEE
ATTN K. Y. HSIEH
ATTN R. M. KOLBAS
DEPT. OF ELEC. ENG.
RALEIGH, NC 27695

PRINCETON UNIVERSITY
ATTN V. J. GOLDMAN
ATTN D. C. TSUI
DEPT. OF ELEC. ENG.
PRINCETON, NJ 08544

US ARMY LABORATORY COMMAND
ATTN TECHNICAL DIRECTOR, AMSLC-TD

INSTALLATION SUPPORT ACTIVITY
ATTN LEGAL OFFICE, SLCIS-CC

USAISC
ATTN TECHNICAL REPORTS BRANCH,
    AMSLC-IM-TR (2 COPIES)

HARRY DIAMOND LABORATORIES
ATTN D/DIVISION DIRECTORS
ATTN CHIEF, SLCHD-NW-E
ATTN CHIEF, SLCHD-NW-EP
ATTN CHIEF, SLCHD-NW-EH
ATTN CHIEF, SLCHD-NW-ES
ATTN CHIEF, SLCHD-NW-R
ATTN CHIEF, SLCHD-NW-TN
ATTN CHIEF, SLCHD-NW-RP
ATTN CHIEF, SLCHD-NW-CS
ATTN CHIEF, SLCHD-NW-TS
ATTN CHIEF, SLCHD-NW-RS
ATTN CHIEF, SLCHD-NW-P
ATTN CHIEF, SLCHD-ST-AP
ATTN CHIEF, SLCHD-ST-SS
ATTN C. S. KENYON, SLCHD-NW-EP
ATTN F. B. MCLEAN, SLCHD-NW-RP
ATTN J. BRUNO, SLCHD-ST-AP (20 COPIES)
ATTN G. HAY, SLCHD-ST-AP
ATTN C. MORRISON, SLCHD-ST-AP (10 COPIES)
ATTN R. NEIFELD, SLCHD-ST-AP
ATTN G. SIMONIS, SLCHD-ST-AP
ATTN M. TOBIN, SLCHD-ST-AP
ATTN D. WORTMAN, SLCHD-ST-AP
ATTN T. BAHDER, SLCHD-ST-AP (20 COPIES)